Fabrication of Nanostructured Thermoelectric Bismuth Telluride Thick Films by Electrochemical Deposition

ARTICLE *in* CHEMISTRY OF MATERIALS · AUGUST 2006

Impact Factor: 8.35 · DOI: 10.1021/cm060171o

7 AUTHORS, INCLUDING:

Muhammet Toprak
KTH Royal Institute of Technology
262 PUBLICATIONS **3,621** CITATIONS
SEE PROFILE

Hesham M. A. Soliman
City Of Scientific Research And Technological…
19 PUBLICATIONS **198** CITATIONS
SEE PROFILE

Jian Zhou
Beihang University(BUAA)
65 PUBLICATIONS **751** CITATIONS
SEE PROFILE

Mamoun Muhammed
KTH Royal Institute of Technology
309 PUBLICATIONS **6,722** CITATIONS
SEE PROFILE

Fabrication of Nanostructured Thermoelectric Bismuth Telluride Thick Films by Electrochemical Deposition

Shanghua Li,*,† Muhammet S. Toprak,†,§ Hesham M. A. Soliman,†,⊥ Jian Zhou,† Mamoun Muhammed,*,† Dieter Platzek,‡ and Eckhard Müller‡

Department of Materials Science and Engineering, Royal Institute of Technology (KTH), SE-100 44 Stockholm, Sweden, and Institute of Materials Research, German Aerospace Center (DLR), D-51170 Köln, Germany

Received January 23, 2006. Revised Manuscript Received April 27, 2006

Bismuth telluride (Bi_2Te_3)-based solid solutions are state-of-the-art thermoelectric (TE) materials for cooling applications at room temperature with a high figure of merit ZT. Nanostructured TE bismuth telluride thick films have been fabricated by electrodeposition from a solution containing bismuth nitrate and tellurium dioxide in 1 M nitric acid onto gold-sputtered aluminum substrates. A conventional three-electrode cell was used with a platinum sheet as the counter electrode and a saturated calomel electrode (SCE) as the reference electrode. Ethylene glycol (EG) was added to the electrolyte in order to increase the thickness of the deposited films, and its effect on the structure, morphology, and compositional stoichiometry of the deposited film was investigated. SEM and XRD were used for structural and compositional characterization. Bismuth telluride films with thicknesses of ca. 350 μm, a stoichiometric composition of Bi_2Te_3, and a hexagonal crystal structure were obtained. A microprobe technique was used to measure the lateral Seebeck coefficient in several samples. The free-standing films were shown to be of high homogeneity, where the abundance distribution of the Seebeck coefficient showed a half width of less than 1 $\mu V\ K^{-1}$ and a high electrical conductivity of around 450 S cm^{-1} at room temperature.

1. Introduction

Thermoelectric (TE) materials are utilized as electric generators or coolers in several applications, such as mini-power-generation systems and microcoolers,[1,2] CCD technology,[3] and infrared detectors.[4] The TE figure of merit, ZT, is expressed as $S^2T\sigma/\lambda$, where S is the Seebeck coefficient, σ is the electrical conductivity, T is the temperature, and λ is the thermal conductivity. Thus, the enhancement of the TE figure of merit can be achieved by increasing S as well as σ or by decreasing λ. Group 15 chalcogenide compounds have received considerable attention for more than three decades because of their potential applications as TE materials. Among the various TE materials, bismuth telluride (Bi_2Te_3), a group 15 chalcogenide compound, has been the main focus of research because of the superior ZT near room temperature in bulk form.[2] By varying the composition, e.g,. with slight deviations from its stoichiometric composition (Bi_2Te_3), bismuth telluride can be tailored to be n-type ($Bi_{2-\delta}Te_{3+\delta}$) or p-type ($Bi_{2+\delta}Te_{3-\delta}$) TE material; the carrier concentration will also be changed, resulting in different TE figures of merit.

Film devices are required to allow for localized cooling at points of interest in many TE applications, such as thermochemistry on a chip, biothermoelectric chips, and active cooling for microelectronic processors.[5] Thin films varying from submicrometer to a few micrometers thick are expected to have thermal conductivity lower than that of the single crystals because of strong phonon scatterings at both surfaces and film interfaces.[6]

The current density value scales with the thickness of the material, and for efficient cooling, a value has to be chosen that achieves an economic operation of a TE device. The optimal current density in a cross-plane arrangement increases with decreasing film thickness, and the Peltier heat flux also increases proportionally. The integration of thin-film TE devices into microsystems was proposed by the microPelt concept[7,8] and focuses on achieving the highest cooling power densities over very small areas (microregions). The use of thick film, on the other hand, is more suitable for application in devices covering large areas and operating at small-to-moderate temperature differences. Thick-film-

* Corresponding author. E-mail: shanghua@mse.kth.se (S.L.); mamoun@matchem.kth.se (M.M.). Tel: 46-8-7908158. Fax: 46-8-7909072.
† Royal Institute of Technology.
§ Present address: Department of Chemistry and Biochemistry, University of California, Santa Barbara, CA 93106.
⊥ Present address: Institute of Advanced Technology and New Materials, Mubarak City for Scientific Research and Technology Applications, New Borg El-Arab City, P.O. Box 21934, Alexandria, Egypt.
‡ German Aerospace Center.

(1) Rowe, D. M. *CRC Handbook of Thermoelectrics;* CRC Press: Boca Raton, FL, 1995.
(2) Rowe, D. M.; Bhandari, C. M. *Modern Thermoelectrics*; Reston: Reston, VA, 1983.
(3) Shafai, C.; Brett, *J. Vac. Sci. Technol., A* **1997**, *15*, 2798.
(4) Min, G.; Rowe, D. M. *Solid-State Electron.* **1999,** *43*, 923.
(5) Hu, Y. F.; Sutter, E.; Si, W. D.; Li, Q. *Appl. Phys. Lett.* **2005**, *87*, 171911.
(6) Hicks, L. D.; Dresselhaus, M. D. *Phys. Rev. B* **1993**, *47*, 12727.
(7) Böttner, H.; Nurnus, J.; Gavriko, A.; Kühner, G.; Jägle, M.; Kunzel, C.; Eberhard, D.; Plescher, G.; Schubert A.; Schlereth, K. H. *J. Microelectromech. Syst.* **2004**, *13*, 414.
(8) Fleurial, J. P.; Snyder, G. J.; Patel, J.; Herman, J. A.; Caillat, T.; Nesmith, B.; Kolawa, E. A. *AIP Conf. Proc.* **2000**, *504* (Space Technology and Applications International Forum Proceedings), 1500.

10.1021/cm060171o CCC: $33.50
Published on Web 07/11/2006

based devices have technological advantages over conventional TE module technology, for which there are practical problems in fabricating pellets with lengths of a few hundred micrometers. On the other hand, there are serious limitations on the use of thin films, if applied to larger areas, due to the need to drain released heat. This problem can be avoided by the use of a thick-film concept, in which the influence of electrical and, in particular, thermal contact and spreading resistance is kept low. Thus, high efficiency and a high coefficient of performance (COP) can be achieved by using thick films with flux quantities that are about 1 order of magnitude larger than those of conventional devices. By controlling the film thickness, it is feasible to ideally tune the flux quantities to the specific application, ensuring efficient operation.

In our previous research,[9,10] we have demonstrated that nanostructuring TE materials reduces the thermal conductivity, λ, thus enhancing their figure of merit, ZT. In addition to the bulk bismuth telluride materials, high-quality bismuth telluride thin films have been fabricated by electrodeposition in an acidic aqueous solution.[11,12] However, no work has been reported on the fabrication of bismuth telluride thick film (100−500 μm). Therefore, there is a need to fabricate nanostructured bismuth telluride thick films.

Several methods have been developed for the fabrication of TE films, such as evaporation,[13] sputtering,[7] MOCVD,[14] and electrodeposition.[15] The electrodeposition technique is an attractive technique because it has many advantages, including cost effectiveness, rapid deposition rates, and relative ease in controlling film thickness from the nanoregime to microregime.

In an earlier study, Takahashi et al.[16] successfully demonstrated electrodeposition of bismuth telluride and confirmed the material's structure by X-ray diffraction (XRD) analysis. A systematic investigation of the electrochemical reactions and compositional changes as a function of applied potential in a nitric-acid bath containing BiO^+ and $HTeO_2^+$ cations was performed by Martin-Gonzalez et al.,[17] and they found that a new mechanism of deposition appears once the potential is more negative than ca. −500 mV. Miyazaki and Kajitani[11] reported that the deposition of either n-type or p-type bismuth telluride could be controlled by controlling the deposition potential. In their studies, the researchers found that n-type bismuth telluride could be obtained at a potential above 20 mV versus a saturated calomel electrode (SCE), whereas p-type bismuth telluride was deposited below 20 mV versus SCE. They proposed that the change in the charge-carrier concentration of bismuth telluride is caused by enhancing the deposition of Bi and decreasing the applied potential during electrolysis. This change in behavior with compositional changes is in agreement with the results of the study by Martin-Gonzalez et al.,[17] even though the potential range reported for the specific bismuth telluride composition was not similar. This difference in potential range was primarily due to the differences in the concentrations of BiO^+ and $HTeO_2^+$ in the electrolytes. However, only simple electrolytes that consisted of BiO^+, $HTeO_2^+$, and HNO_3 were employed in the above studies, and the thickness of the films was limited to less than 200 μm because of a decrease in the electrical conductivity of the deposited films over metal substrates and poor adhesion between films and substrates.

Various organic additives in relatively small addition amounts have been shown to have large effects on the physical properties of electrodeposited films, such as brightness, smoothness, hardness, and ductility.[18,19] Organic solvents, pure as well as in a mixture, are increasingly used in electrodeposition processes.[20,21] The use of organic solvents as additives in the electrolytes results in changing the mechanism of the electrodeposition process, which makes it possible to develop films with greater thickness, e.g., 200−500 μm. In this paper, we report on the fabrication of nanostructured thick films of bismuth telluride by an electrodeposition technique. The effect of adding an organic solvent, ethylene glycol (EG), to the electrolyte has on the structure, morphology, and compositional stoichiometry of the deposited bismuth telluride film has been investigated. This work also creates the possibility of preparing nanostructured TE bismuth telluride with different stoichiometries either attached on substrates or as free-standing films.

2. Experimental Section

Film Fabrication. Thick films of bismuth telluride were cathodically deposited onto gold sputtered-aluminum substrates. A gold layer (~100 nm thick) was sputtered onto one side of a piece of aluminum foil (0.1 mm thick, $1.5 \times 1.5 = 2.25$ cm^2, Riedel-de Haën) to serve as the working electrode (cathode) for electrodeposition. The electrolyte contained 0.013 M BiO^+ and 0.01 M $HTeO_2^+$ in 1 M HNO_3, where the concentration was determined on the basis of work by Miyazaki et al.[11] and the ratio between bismuth and tellurium was that according to Sapp et al.[22] Various amounts of EG were added to the electrolyte at concentrations of 10, 20, 30, and 40% (v/v) to study the organic-solvent effect on bismuth telluride thick-film formation. A three-electrode conventional electrochemical cell was used for the deposition of bismuth telluride with Pt foil (~8 cm^2) as the counter electrode (anode) and SCE as the reference electrode with a cathode−anode separating distance of 2 cm. Ar gas was bubbled into the electrolyte for 10 min to

(9) Toprak, M. S.; Stiewe, C.; Platzek, D.; Williams, S.; Bertini, L.; Müller, E.; Gatti, C.; Zhang, Y.; Rowe, M.; Muhammed, M *Adv. Funct. Mater.* **2004**, *14*, 1189.
(10) Stiewe, C.; Bertini, L.; Toprak, M. S.; Christensen, M.; Platzek, D.; Williams, S.; Gatti, C.; Müller, E.; Iversen, B. B.; Muhammed, M.; Rowe, D. M. *J. Appl. Phys.* **2005**, *97*, 1.
(11) Miyazaki, Y.; Kajitani, T. *J. Cryst. Growth* **2001**, *229*, 542.
(12) Fleurial, J. P.; Olson, N. T.; Borshchevsky, A.; Caillat, T.; Kolawa, E.; Ryan, M. A.; Philips, W. M. U.S. Patent, 6 288 321, 2001.
(13) Zou, H.; Rowe, D. M.; Min, G. *J. Vac. Sci. Technol., A* **2001**, *19*, 899.
(14) Venkatasubramanian, R.; Colpitts, T.; Watko, E.; Lamvik, M.; El-Masry, N. *J. Cryst. Growth* **1997**, *170*, 817.
(15) Takahashi, M.; Muramatsu, Y.; Suzuki, T.; Sato, S.; Watanabe, M.; Wakita, K.; Uchida, T. *J. Electrochem. Soc.* **2003**, *150*, C169.
(16) Takahashi, M.; Katou, Y.; Nagata, K.; Futura, S. *Thin Solid Films* **1994**, *240*, 70.
(17) Martin-Gonzalez, M. S.; Prieto, A. L.; Gronsky, R.; Sands, T.; Stacy, A. M. *J. Electrochem. Soc.* **2002**, *149*, C546.
(18) Cofre, P.; Bustos, A. *J. Appl. Electrochem.* **1994**, *24*, 564.
(19) Campbell, S. A.; Farndon, E. E.; Walsh, F. C.; Kalaji, M. *Trans. Inst. Met. Finish.* **1997**, *75*, 10.
(20) Soliman, H. M. A. *Appl. Surf. Sci.* **2002**, *195*, 155.
(21) Sultan, S.; Tikoo, P. K. *Surf. Technol.* **1984**, *22*, 241.
(22) Sapp, S. A.; Lakshmi, B. B.; Martin, C. R. *Adv. Mater.* **1999**, *11*, 402.

remove oxygen from the solution prior to the electrodeposition and was continued throughout the experiment at a low rate (~10 mL/min). Electrodeposition was carried out using an EG&G PAR model 263A potentiostat/galvanostat at room temperature (~298 K) either potentiostatically or galvanostatically with regular monitoring of the cathodic current and potential, respectively. The potentiostatic electrodeposition was performed at −50, −75, −120, −150, and −200 mV, as these values are within the common diffusion-controlled region between all used solutions.[20] For the galvanostatic electrodeposition, a current density of 3.3 mA/cm^2 was used while a high potential of around 1.9 V between the cathode and the anode was applied. Typical electrodeposition duration was around 24 h. Finally, the deposited films were removed from the electrolyte and rinsed in three steps; 0.1 M HNO_3 solution (pH ~1), deionized water, and ethanol, followed by drying in air.

XRD patterns of the films were obtained using a Philips PW 1012/20 and 3020 diffractometer with Cu Kα radiation. The average crystallite size, D, could be calculated from the peak broadening of the diffraction pattern using Scherrer's equation,[23] $D = 0.9\lambda/(\beta\cos\theta)$, where β is the pure diffraction line width, full width at half-maximum, and λ is the X-ray wavelength (Cu Kα_1, λ = 1.54056 Å).

Electrodeposited bismuth telluride thick films were imaged with both transmission electron microscopy (TEM, JEOL 2000EX) and scanning electron microscopy (SEM, JEOL JSM-888) equipped with an energy-dispersive X-ray spectrometer (EDS), which was used for composition analysis. The thickness of the films was determined by measuring the cross-section of the film under SEM.

TE Evaluation. Seebeck coefficient and electrical conductivity of different samples prepared by the electrodeposition process have been measured. The Seebeck microprobe (SMP) is a device for measuring the Seebeck coefficient on the sample surface with a spatial resolution down to 10−50 μm (depending on the thermal conductivity of the material).

A heated probe tip is positioned onto the sample surface. The sample is fixed in good electrical and thermal contact to a heat sink and is connected to another thermocouple measuring the sink temperature. The heat flow from the probe tip to the sample causes a local temperature gradient in the vicinity of the tip. Mounting the probe to a three-dimensional micropositioning system allows for the determination of the thermopower at each microposition of the sample surface. The result is a two-dimensional image of the Seebeck coefficient.[24,25] Special sample holders have been developed to mechanically fix thick films as well ensure simultaneously good electrical and thermal contact as a precondition for a high-quality measurement. The SMP apparatus has been improved by adding an electronic contact detection system so that the probe tip will stop its movement immediately after touching the sample to avoid destruction of the films.

Seebeck coefficient measurement is a tool to detect the distribution of different electrically active components in the materials. It is capable of detecting functional inhomogeneities, different phases, even small differences in doping concentration, which cannot be detected by other surface analysis methods such as SEM, EDS, etc. Measuring the Seebeck coefficient of films can be difficult, because the local temperature gradient caused by the probe tip can also heat the materials of the supporting substrate, yielding an integration of the Seebeck coefficient of the sample and the substrate. If the substrate has a very low thermal coupling, this effect will be negligible. The TE thick films were deposited on a Au-coated Al substrate with a very good thermal coupling, which could lead to erroneous measurements. Taking into account the thickness of the samples of more than 100 μm, this effect will disappear or at least attenuate, because the local temperature gradient will not exceed a certain depth of an estimated 50 μm in bismuth telluride. Recent results show that it is indeed now possible to measure the influence of a substrate and estimate the depth of a temperature gradient.[26]

The electrical conductivity has been measured by means of an in-line four-point probe between room temperature and 300 °C. An ac current of several milliamps is applied to the outer contact probes, and the voltage is measured with the inner probes. The distance between all adjacent probes is equal. A numerical correction factor (Valdez factor) is applied to take into account the particular geometry of the sample. To eliminate the influence of the metallic substrate on the electrical conductivity measurement, we considered only free-standing films in this work. Because the toughness of the deposited free-standing films is not high enough, it is difficult to apply the four-point probe without destroying the film. Therefore, electrical conductivity measurement was limited to several free-standing films that occasionally possess better toughness. A more accurate method for measuring electrical conductivity on thick films is currently under study.

3. Results and Discussion

Synthesis and Fundamental Characterization. The electrodeposition process of bismuth telluride was well-investigated.[11,27,28] In both potentiostatic and galvanostatic electrodeposition processes, bismuth and tellurium compounds are dissolved in nitric acid to form the oxide cations BiO^+ and $HTeO_2^+$. Bismuth telluride is insoluble in dilute nitric acid; thus, reduction of $HTeO_2^+$ to Te^{2-} at an electrode will result in the precipitation of Bi_2Te_3 on the electrode surface. This can take place in a potentiostatic electrodeposition process, because BiO^+ requires a lower potential than $HTeO_2^+$ and is thus more difficult to reduce.[27] The overall reaction for the process is

$$13H^+ + 18e^- + 2BiO^+ + 3HTeO_2^+ \rightarrow Bi_2Te_3\downarrow + 8H_2O \quad (1)$$

However, for a galvanostatic electrodeposition process, especially with high potential (>1.5 V) between the two electrodes, BiO^+ and $HTeO_2^+$ will be reduced simultaneously, resulting in a solid-state reaction between Bi and Te in the molecular range. The electrodeposition process of Bi_2Te_3 can be expressed by the following steps.[28] First, the ions from the bulk electrolyte diffuse to the electrode surface and are absorbed on the growth sites at the electrode surface. The absorbed ions are then reduced at the cathode. These

(23) Klug, H. P.; Alexander, L. E. *X-ray Diffraction Procedures*; John Wiley & Sons Inc.: New York, 1954.
(24) Reinshaus, P.; Süssmann, H.; Bohm, M.; Schuck, A.; Dietrich, T. *Proceedings of the 2nd European Symposium on Thermoelectrics: Materials, Processing Techniques, and Applications*, Sept 15−17, 2004, Krakow, Poland; European Thermoelectric Society; p 90.
(25) Platzek, D.; Zuber, A.; Stiewe, C.; Bähr, G.; Reinshaus, P.; Müller, E. *Proceedings of the 22nd International Conference on Thermoelectrics*, LaGrande-Motte, France, Aug 17−21, 2003; IEEE: New York, 2004; p 528.
(26) Platzek, D.; Karpinski, G.; Stiewe, C.; Ziolkowski, P.; Stordeur, M.; Engers, B.; Müller, E. *3rd European Conference on Thermoelectrics*, Nancy, France, Sept 1−2, 2005; European Thermoelectric Society.
(27) Fleurial, J. P.; Borshchevsky, A.; Ryan, M. A.; Phillips, W. M.; Snyder, J. G.; Caillat, T.; Kolawa, E. A.; Herman, J. A.; Mueller, P.; Nicolet, M. *Mater. Res. Soc. Symp. Proc.* **1998**, *545*, 493.
(28) Jin, C.; Xiang, X.; Jia, C.; Liu, W.; Cai, W.; Yao, L.; Li, X. *J. Phys. Chem. B* **2004**, *108*, 1844.

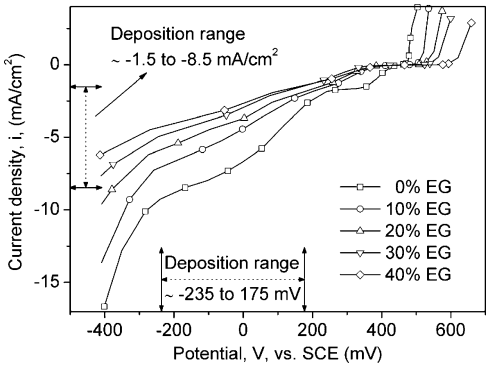

Figure 1. Potential−current relation of Au-sputtered Al substrate in 1 M HNO_3, 0.013 M BiO^+, and 0.01 M $HTeO_2^+$ solution at 298 K in the absence and presence of 10−40% (v/v) EG.

two steps have been used for controlling the composition of prepared films and are chemically presented in the following two equations

$$BiO^+ + 2H^+ + 3e^- \rightarrow Bi(s) + H_2O \quad (2)$$

$$HTeO_2^+ + 3H^+ + 4e^- \rightarrow Te(s) + 2H_2O \quad (3)$$

Third, the reduced Bi and Te atoms react by a solid-state reaction to form Bi_2Te_3. This step mainly affects the crystalline nature of the deposits and is expressed as follows

$$2Bi(s) + 3Te(s) \rightarrow Bi_2Te_3(s) \quad (4)$$

Figure 1 shows the potential−current curves for the solution containing 1 M HNO_3, 0.013 M BiO^+, and 0.01 M $HTeO_2^+$ in the absence and presence of different amounts of EG (10−40% (v/v)). No further addition of ethylene glycol is necessary, because the effect of both 30 and 40% (v/v) is almost overlapped, as shown in Figure 1. The limiting current region is observed between $E = -275$ mV and $E = +75$ mV for the solution without EG, whereas it is between $E = -235$ mV and $E = +175$ mV in the presence of EG. The potential range (in the absence of EG) is not in agreement with that suggested by Miyazaki et al.[11] It is noticeable in Figure 1 that the open circuit potential increases toward the more noble direction and that the limiting current density decreases as EG is added to the electrolyte. The same trend prevails as the concentration of EG increases.

Bismuth telluride thick films are obtained by both potentiostatic and galvanostatic routes on the basis of the potential−current values as shown in Figure 1. Table 1 summarizes the different electrodeposition conditions for all electrolytes at 298 K, considering the 0% EG solution to be the solution containing 1 M HNO_3, 0.013 M BiO^+, and 0.01 M $HTeO_2^+$. The color of the films is found to depend on the applied potential; it changes from gray at lower potentials into black at higher potentials. The face in contact with the substrate exhibits a uniform surface with metallic luster. Although several other substrate materials have been tested (Cu, Ni, Si, and stainless steel), adhesion of the deposited films and mechanical quality have been found to be the best for Au-sputtered Al substrate. Thus, Au-sputtered Al substrate is used for all of the film studies presented in this paper. The adhesion of the deposited bismuth telluride films to the substrate varies from excellent at −50 mV to poor at −200 mV in the case of solution without EG, whereas the opposite behavior is observed in the presence of EG. However, poor adhesion resulting in an easy separation between deposited films and substrate without breaking the films can be used to fabricate free-standing films. On the other hand, excellent adhesion results in the feasibility of forming thicker films.

Table 1. Summary of Electrodeposition Conditions for Bismuth Telluride Thick Films

electrolytic solution	applied potential (mV)	deposition time (h)	adhesion	stoichiometry	average film thickness (μm)	color
			Potentiostat			
0 EG	−50	24	excellent	$Bi_{1.9}Te_{3.1}$	180	gray
	−75	24	very good	$Bi_{1.95}Te_{3.05}$	150	gray
	−120	24	good	Bi_2Te_3	100	black
	−150	24	fair	$Bi_{2.1}Te_{2.9}$	100	black
	−200	24	poor	$Bi_{2.2}Te_{2.8}$	100	black
10 EG	−50	24	poor	$Bi_{2.2}Te_{2.8}$	150	grey
	−75	24	excellent	Bi_2Te_3	200	grey
	−120	24	poor	$Bi_{2.7}Te_{2.3}$	150	grey
	−150	24	poor	$Bi_{2.7}Te_{2.3}$	170	black
	−200	24	poor	$Bi_{2.7}Te_{2.3}$	180	black
20 EG	−50	24	excellent	$Bi_{1.9}Te_{3.1}$	180	grey
	−75	24	excellent	$Bi_{1.95}Te_{3.05}$	180	grey
	−120	24	excellent	Bi_2Te_3	180	black
	−150	24	excellent	Bi_2Te_3	180	black
	−200	24	excellent	$Bi_{2.05}Te_{2.95}$	180	black
30 EG	−50	24	excellent	$Bi_{1.4}Te_{3.6}$	180	grey
	−75	24	very good	$Bi_{1.5}Te_{3.5}$	180	grey
	−120	24	good	Bi_2Te_3	200	black
	−150	24	good	Bi_2Te_3	200	black
	−200	24	good	$Bi_{2.2}Te_{2.8}$	200	black
40 EG	−50	24	excellent	Bi_2Te_3	160	grey
	−50	48	excellent	Bi_2Te_3	300	grey
	−75	24	excellent	Bi_2Te_3	200	black
	−120	24	very good	Bi_2Te_3	250	black
	−150	24	very good	Bi_2Te_3	300	black
	−200	24	very good	Bi_2Te_3	300	black
			Galvanostatic			
0 EG	3.3	24	poor	Bi_2Te_3	240	grey
	3.3	48	fair	Bi_2Te_3	190	grey
	7.5	24	excellent	Bi_2Te_3	100	black
10 EG	3.3	24	poor	Bi_2Te_3	100	grey
	3.3	48	poor	Bi_2Te_3	120	grey
	6	24	poor	$Bi_{2.7}Te_{2.3}$	150	grey
20 EG	3.3	24	excellent	Bi_2Te_3	180	grey
	3.3	48	excellent	Bi_2Te_3	350	grey
	4.5	24	excellent	Bi_2Te_3	180	black
30 EG	3.3	24	excellent	Bi_2Te_3	180	grey
	3.3	48	excellent	Bi_2Te_3	180	black
	3.5	24	excellent	Bi_2Te_3	200	black
40 EG	3	24	excellent	Bi_2Te_3	250	black
	3	48	excellent	Bi_2Te_3	300	black

The thickness of the deposited films decreases with increasing the applied potential when the electrodeposition is carried out in aqueous solutions without EG, whereas it increases with the addition of EG. The maximum thickness of free-standing films achieved here is around 240 μm (see Figure 2A), obtained in the case of galvanostatic electrodeposition without EG at 3.3 mA/cm^2 (∼1.9 V) for 24 h, whereas the maximum thickness of films adhering well to the substrate is found to be around 350 μm (see Figure 2B), in the case of 20% (v/v) EG at 3.3 mA/cm^2 (∼1.9 V) for 48 h. Thicker free-standing films cannot be obtained just by increasing the time of electrodeposition process because of the adhesion problem. The increase in thickness by using EG as an additive in the electrolyte is attributed to the promotion of the adhesion of as-deposited bismuth telluride to the substrate. As for the adhesion enhancement by using

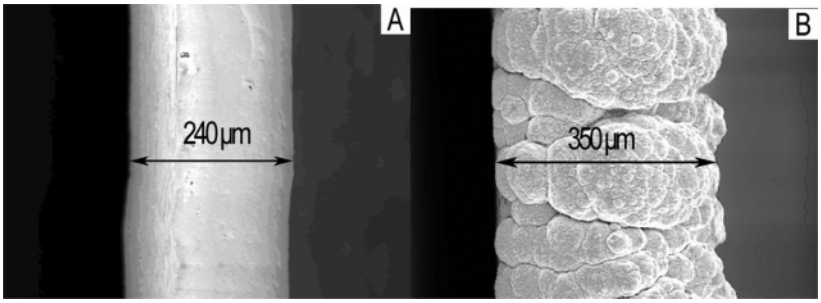

Figure 2. SEM images of the films in edge view showing the thickness of: (A) 240 μm for the free-standing film after deposition for 24 h in the absence of EG and (B) 350 μm for the bismuth telluride film attached to the substrate after deposition for 48 h in the presence of EG. (Both films are as-deposited at 298 K from 1 M HNO_3, 0.013 M BiO^+, and 0.01 M $HTeO_2^+$ with a current density of 3.3 mA/cm^2.)

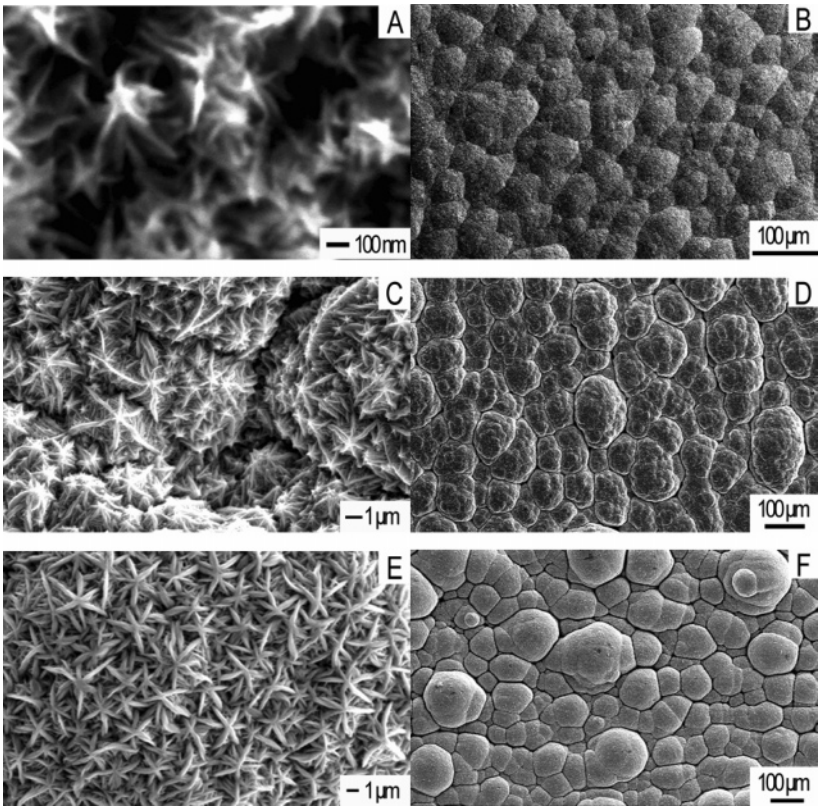

Figure 3. SEM images of galvanostatically electrodeposited bismuth telluride films of (A, B) stoichiometry from 1 M HNO_3, 0.013 M BiO^+, and 0.01 M $HTeO_2^+$ without EG in the electrolyte; (C, D) stoichiometry from 1 M HNO_3, 0.013 M BiO^+, and 0.01 M $HTeO_2^+$ with EG in the electrolyte; and (E, F) nonstoichiometry from 1 M HNO_3, 0.008 M BiO^+, and 0.01 M $HTeO_2^+$ without EG in the electrolyte. (All films are as-deposited at 298 K with a current density of 3.3 mA/cm^2.)

EG, it refers to the high viscosity of EG, which slows down the movement of the ions (as shown in Figure 1), leading to smooth deposition on the electrode surface; as a result, the adhesion is promoted.[20]

SEM images in Figure 3 clearly show that in galvanostatic electrodeposition, the morphology of electrodeposited bismuth telluride films depends on the composition of the electrolyte and stoichiometry of the films, which is in agreement with Martin-Gonzalez et al.[17] Needlelike structures with very small features in the nanorange ($\sim$20$-$30 nm in width) are observed on stoichiometric films in the absence of EG (see Figure 3A), whereas interconnected needlelike structures are found on stoichiometric films in the presence of EG (see Figure 3C). However, nonstoichiometric films fabricated by increasing the ratio between BiO^+ and $HTeO_2^+$ in the original electrolyte exhibit free starlike structures (see Figure 3E). Panels B, D, and F in Figure 3 show that stoichiometric films in the presence (D) and absence (B and F) of EG have the most-compact structures. In potentiostatic electrodeposition, the morphology of electrodeposited bismuth telluride films is strongly affected by deposition potentials and the composition of the electrolyte. Needlelike structures are observed on the electrodeposited films in the absence of EG at $-$120 mV (see Figure 4A) and 30$-$40% (v/v) EG at $-$120 mV (see panels D and F of Figure 4), whereas at the same deposition potential of $-$120 mV, a round needlelike structure that looks like lettuce leaves is formed from 20% (v/v) EG (Figure 4C). In the case of 10% (v/v) EG at $-$75 mV and 40% (v/v) EG at $-$75 mV, straight hexagonal and rounded hexagonal structures are formed (see panels B and F of Figure 4), respectively. Contrary to many authors'[15,17] statements that different stoichiometries form dissimilar structures, it is found in this investigation that there is no relation between the stoichiometry and the structure.

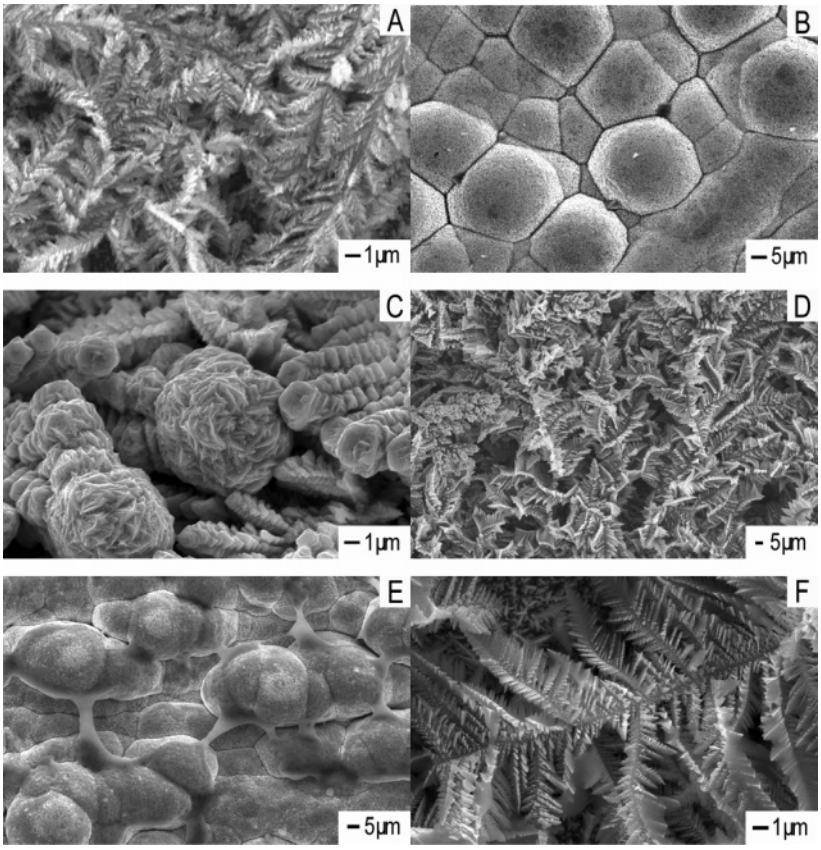

Figure 4. SEM images of bismuth telluride films electrodeposited of 24 h at 298 K from 1 M HNO_3, 0.013 M BiO^+, and 0.01 M $HTeO_2^+$ at (A) 0% EG, −120 mV; (B) 10% EG, −75 mV; (C) 20% EG, −120 mV; (D) 30% EG, −120 mV; (E) 40% EG, −75 mV; and (F) 40% EG, −120 mV.

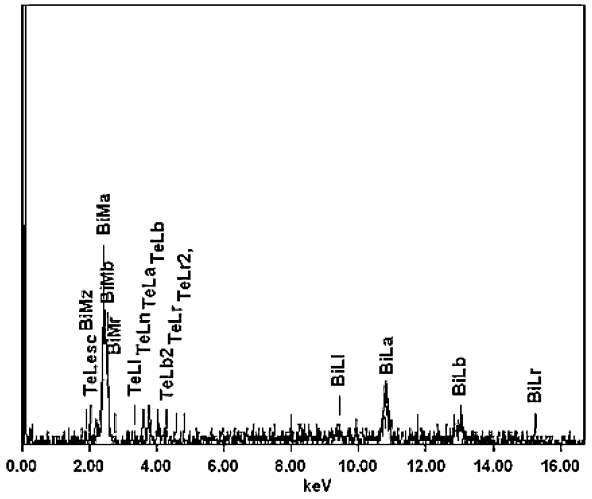

Figure 5. EDS spectrum of stoichiometric bismuth telluride films electrodeposited after 24 h at 298 K from 1 M HNO_3, 0.013 M BiO^+, and 0.01 M $HTeO_2^+$ with a current density of 3.3 mA/cm^2 in absence of EG.

The statement that the formation of n-type or p-type bismuth telluride is related to the microstructure rather than to stoichiometry[29] is supported by the results of this work. It is important to take into account that the last statement applies only at a higher deposition potential that is accompanied by cathodic hydrogen evolution, where dendritic structure prevails.

The typical EDS result is presented in Figure 5, which verifies that the films deposited galvanostatically with a current density of 3.3 mA/cm^2 consist of Bi and Te, and a quantitative analysis of the spectrum indicates that the Bi:Te atomic ratio is close to 2:3. However, the stoichiometry of the potentiostatically deposited bismuth telluride is dependent on the applied potential as well as the electrolyte composition with a stoichiometric variation range of $Bi_{1.4-2.7}Te_{3.6-2.3}$. Table 1 illustrates that the stoichiometric composition is achieved at −120 and −150 mV from solutions in the absence and presence of 30% (v/v) EG, at −75 mV in the presence of 10% (v/v) EG, and at all deposition potentials in the presence of 20 and 40% (v/v) EG. The stoichiometry of films obtained potentiostatically exhibit no coherent and logical evolution. From EDS, the distribution of both Bi and Te for all the films is homogeneous, indicating that the prepared films have a good tolerance to the experimental conditions.

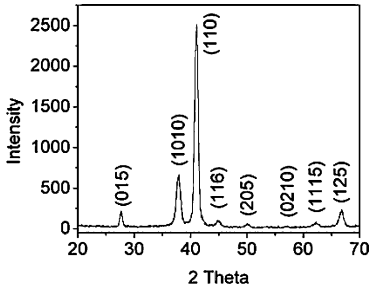

Figure 6. XRD pattern of as-deposited bismuth telluride thick film after 24 h at 298 K from 1 M HNO_3, 0.013 M BiO^+, and 0.01 M $HTeO_2^+$ with a current density of 3.3 mA/cm^2 in the absence of EG.

Figure 6 shows the XRD pattern of an example of the electrodeposited bismuth telluride thick films. The XRD

(29) Bentien, A.; Paschen, S.; Plotner, M.; Grafe, H.; Fisher, W. J. *J. Solid State Electrochem.* **2003**, *7*, 714.

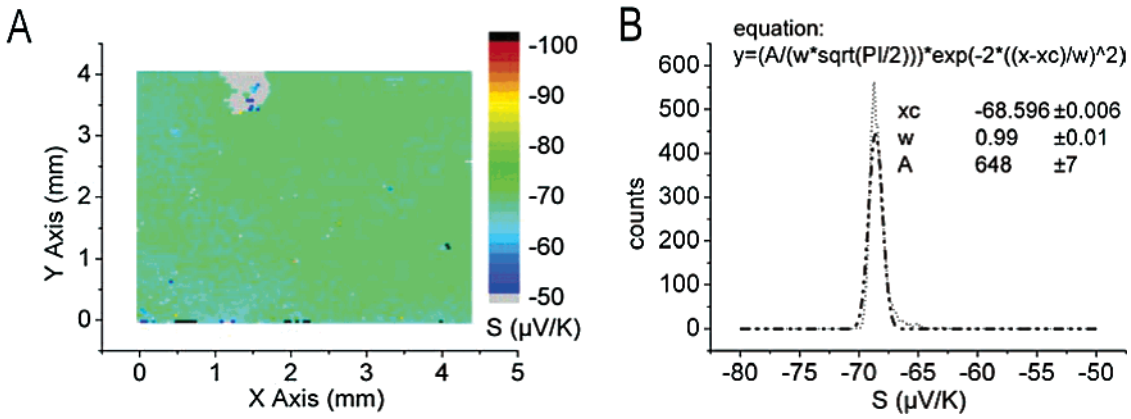

Figure 7. (A) Spatial distribution of the Seebeck coefficient measured on as-deposited bismuth telluride thick film after 24 h at 298 K from 1 M HNO_3, 0.013 M BiO^+, and 0.01 M $HTeO_2^+$ with a current density of 3.3 mA/cm^2 in the absence of EG, and (B) the abundance distribution showing very high homogeneity indicated by the half width of less than 1 μV K^{-1}.

pattern exhibits polycrystalline bismuth telluride in the as-deposited state with (110) as the prominent plane parallel to the substrate. According to the standard ICDD PDF card (08-0021), all of the detected peaks are indexed as those from the rhombohedral Bi_2Te_3 crystal (space group ($R\bar{3}$ m) (166)) with hexagonal crystal structures. However, the intensity ratios of the peaks are not in good agreement with those obtained by XRD on a ground product, indicating an orientational effect in the film growth.[30] The average crystallite size of electrodeposited bismuth telluride calculated by Scherrer's equation is in the range between 10 and 30 nm, which is consistent with the result from SEM as shown in Figure 3A.

TE Properties. The measured Seebeck coefficient of different deposited stoichiometric Bi_2Te_3 thick films is between −68 and −85 μV K^{-1}, which shows that the material is n-type and is higher in absolute value than other reported undoped bismuth telluride films (from −40 to −60 μV K^{-1}) prepared by electrodeposition at room temperature.[11,27,31] Figure 7A shows the spatial distribution of the Seebeck coefficient measured on a typical electrodeposited bismuth telluride thick film with a thickness of around 200 μm. It is obvious that the as-deposited bismuth telluride thick film has a very high homogeneity in the Seebeck coefficient and the abundance distribution shows a half width of less than 1 μV K^{-1} at an average Seebeck coefficient of −68 μV K^{-1}, as seen from Figure 7B. As it has been reported that annealing increases thermopower and resistivity consistently with a decrease in carrier concentration,[31] the as-deposited films have been annealed at 300 °C for 2 h under an inert atmosphere; an average Seebeck coefficient of −125 μV K^{-1} has been obtained, as seen from Figure 8.

The free-standing stoichiometric Bi_2Te_3 films deposited galvanostatically in the absence of EG possess high electrical conductivity of around 450 S cm^{-1} at room temperature and show a slightly lower electrical conductivity when heated to higher temperatures up to 300 °C. Thereafter, when the films are cooled, the electrical conductivity increases with decreasing temperature to a higher level than when at room temperature previously, which might indicate a microstructural change in the film. Therefore, the power factor ($S^2\sigma$) of the free-standing stoichiometric Bi_2Te_3 films can be calculated to be around 200 μW m^{-1}K^{-2} at room temperature and will increase to around 600 μW m^{-1} K^{-2} at 300 °C. Thermal conductivity is still under investigation, although it is difficult to measure for films.

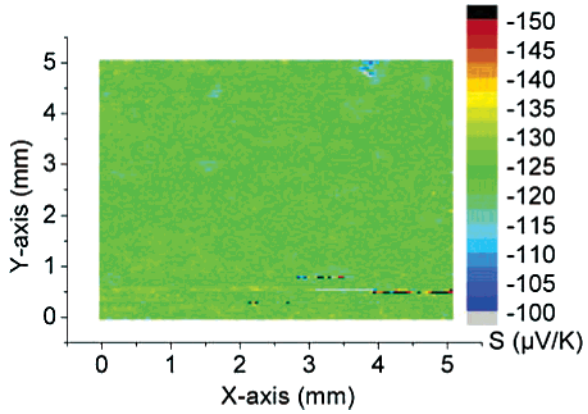

Figure 8. Spatial distribution of the Seebeck coefficient measured on films after annealing at 300 °C for 2 h under an inert atmosphere.

4. Conclusions

Nanostructured TE bismuth telluride thick films with a thickness up to 350 μm have been fabricated by electrodeposition. The influence of EG dissolved in the electrolyte on the structure, morphology, and compositional stoichiometry of the deposited films has been investigated. The films possess polycrystalline Bi_2Te_3 hexagonal unit cells with an average crystallite size of around 10−30 nm. A high homogeneity of the Seebeck coefficient and a high electrical conductivity resulting in a high power factor ($S^2\sigma$) at room temperature have been achieved on the fabricated thick films.

Acknowledgment. This work was supported by the European Community under Contract FP6-512805, the IMS project, and the Swedish Research Council (Vetenskapsrådet).

CM060171O

(30) Chaouni, H.; Magri, P.; Bessieres, J.; Boulanger, C.; Heizmann, J. J. *Proc. ICOTOM 10, Mater. Sci. Forum* **1994**, 1371.
(31) Stoltz, N. G.; Snyder, G. J. *Proceedings of the 21st International Conference on Thermoelectrics*, Long Beach, CA, Aug 25−29, 2002; IEEE: New York, 2002; p 28.